Two new μ_2-(1,1-Azido) and μ_2-(1,1-Phenoxido)-Bridged Dinuclear Nickel(II) Complexes: Syntheses, Single-Crystal Structures and Magnetic Studies

Samar Dolai,[a] Soumen Manna,[a] Albert Figuerola,*[,b,c] Hyuma Masu,[d] Subal Chandra Manna*[,a]

[a]*Department of Chemistry and Chemical Technology, Vidyasagar University, Midnapore 721102, West Bengal, India, E-mail: scmanna@mail.vidyasagar.ac.in, Fax: (91) (03222) 275329.*

[b]*Departament de Química Inorgànica i Orgànica, Secció de Química Inorgànica, Universitat de Barcelona, MartíiFranquès 1-11, 08028 Barcelona, Spain.*

[c]*Institut de Nanociència i Nanotecnologia (IN2UB), Universitat de Barcelona, Martí i Franquès 1-11, 08028 Barcelona, Spain.*

[d]*Center for Analytical Instrumentation, Chiba University, 1-33 Yayoi-cho, Inage-ku, Chiba 263-8522, Japan.*

Abstract

Two dinuclear azido bridged Ni(II) complexes $[Ni_2(HL^1)_2(N_3)(C_8H_7O_3)]\cdot(H_2O)$ (**1**) and $[Ni_2(L^2)_2(N_3)_2(H_2O)]$(**2**) [$H_2L^1$ and HL^2 are Schiff bases, obtained from the condensation of 2-hydroxy-3-methoxy-benzaldehyde with 2-amino-2-methyl-1-propanol and N,N-diethylethylene diammine, respectively; $C_8H_7O_3$ = 3-methoxy-2-oxo-benzaldehyde] have been synthesized and their crystal structures have been determined. Complex **1**, $C_{32}H_{39}N_5Ni_2O_{10}$, crystallizes in a triclinic system, space group *P*-1 with a = 10.0846(6), b = 12.5179(7), c = 14.1176(8) Å, α = 74.3873(7), β =83.9553(7), γ = 83.1921(7) º and Z = 2; complex **2**, $C_{28}H_{44}N_{10}Ni_2O_5$, crystallizes in an orthorhombic system, space group Pbca with a = 12.4197(1), b = 21.4737(4), c = 24.4569(5) Å, and Z = 8. X-ray single crystal structure determination reveals that both the complexes are dinuclear with μ_2-(1,1-azido) and μ_2-(penoxido) bridges. Variable temperature magnetic studies indicate overall ferromagnetic interaction between nickel(II) centers in both the

complexes. The experimental magnetic data of the complexes were fitted using PHI program and isotropic Hamiltonian $H = -JS_1S_2$, where $S_1 = S_2 = S_{Ni}$. A zero-field splitting parameter (D) and intermolecular interaction term (zJ') were also considered in the model and a good agreement between experimental and simulated curves were found by using the following parameters: g_{Ni}= 2.13, D_{Ni}= 5.83 cm^{-1}, $J_{Ni\text{-}Ni}$ = 14.61 cm^{-1} and zJ' = -0.1 cm^{-1} for **1**, and g_{Ni}= 2.15, D_{Ni}= 2.33 cm^{-1}, $J_{Ni\text{-}Ni}$ = 13.09 $cm^{-1}$and zJ' = -0.07 cm^{-1} for **2**.

Keywords: Dinuclear nickel(II) complex; End-on-azide bridges; Phenoxido bridges; Crystal structures; Magnetic properties.

1. Introduction

Short span ligand bridged polynuclear nickel complexes are important due to their interesting structure and potential application as magnetic materials [1-2]. Among the various nickel complexes, phenoxido bridged and N,N,O donor Schiff base coordinated dinuclear nickel(II) complexes are widely studies due to their interesting magnetic properties and their potentially to function as structural, catalytic and electronic models for the enzyme urease [3-4]. 2-hydroxy-3-methoxy benzaldehyde derived N,N,O donor tridentate Schiff bases and short span bridging anionic ligand like azide, cyanate, thiocyanate etc. is a useful combination for the synthesis of dinuclear nickel complexes [5]. Among the anionic ligands, azide has versatile coordination modes and functions as suitable superexchange pathway between the paramagnetic metal centres [6]. It is to note that generally μ-(1,3-N_3) bridging azide results antiferromagnetic coupling whereas that of μ-(1,1-N_3) bridging results ferromagnetic interaction [7]. Phenoxido (μ-O) and μ-(1,1-N_3)-azido bridged is an important combination for desigining dinuclear nickel(II) compound based magnetic materials [8]. It is interesting to note that phenoxido-

bridged dinuclear nickel complexes show ferromagnetic coupling if the Ni-O-Ni angle is less than 97º, whereas show antiferromagnetic coupling if the angle is greater than 97º [9]. Literature survey reveals that a few dinuclear complexes with phenoxido and μ-(1,1-N_3)-azido complexes are reported in the literature. Bridging Ni-O-Ni and Ni-N-Ni angles depend on the choice of the chelating Schiff ligand and magnetic behavior of the compound controlled by these bond angles [8]. These phenomenon promoted us to synthesize phenoxido and μ-1,1-azido bridged dinuclear nickel complexes using new tridentate Schiff base ligands. In the present contribution we have used 2-hydroxy-3-methoxy benzaldehyde based Schiff bases, 2-[(2-Hydroxy-1,1-dimethyl-ethylimino)-methyl]-6-methoxy-phenol (H_2L^1) and 2-[(2-Diethylamino-ethylimino)-methyl]-6-methoxy-phenol (HL^2) and synthesized two dinuclear nickel complexes, $[Ni_2(L^1)_2(\mu_{1,1}\text{-}N_3)(C_8H_7O_3)]\cdot H_2O$ (**1**) and $[Ni_2(L^2)_2(\mu_{1,1}\text{-}N_3)(N_3)(H_2O)]$ (**2**). Variable temperature magnetic property studies show overall ferromagnetic interaction in both the complexes.

2. Experimental

2.1. Materials and methods

High purity N,N-diethylethylenediammine and 2-amino-2-methyl-1-propanol of Aldrich Chemical Co. Inc. were used and all other chemicals were of AR grade.

Perkin-Elmer 240C elemental analyzer was used for elemental analyses (C, H, N). Bruker Vector 22 FT IR spectrophotometer was used for recording IR spectra (as KBr pellets) in the range 400 to 4000 cm^{-1}. Room temperature electronic spectra of the complexes were recorded with Shimadzu UV-1601 UV-vis spectrophotometer. Quartz cuvettes with a 1 cm path length and a 3 cm^3 volume were used for all measurements.

2.2. Synthesis of complexes

The complexes have been synthesized by adopting the procedures schematically given in Scheme 1.

Scheme 1 Synthesis of **1** and **2**.

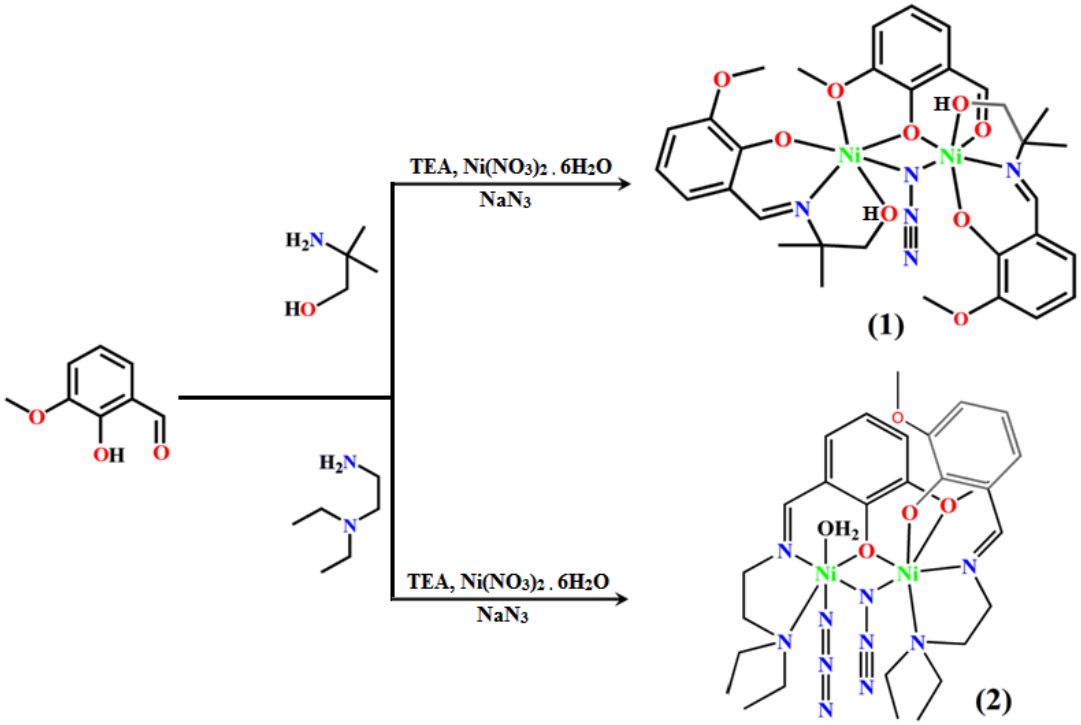

Scheme 1 Synthesis of **1** and **2**.

*2.2.1. $[Ni_2(HL^1)_2(N_3)(C_8H_7O_3)]\cdot(H_2O)$ (**1**)*

Methanolic solution (15 mL) of mixture of 2-amino-2-methyl-1-propanol (1 mmol, 0.089 g) and 2-hydroxy-3-methoxy-benzaldehyde (1 mmol, 0.152 g) was refluxed (at 60 ºC) for 1 h, and the solution is cooled to room temperature (at 27 ºC). Solid nickel nitrate hexahydrate (0.290 g, 1 mmol) was added to this solution under stirring condition, and then an aqueous solution (2 mL) of NaN_3 (1 mmol, 0.065 g) was added. The resulting green color reaction mixture was stirred for

1h and filtered, and the filtrate was kept in a refrigerator for slow evaporation. Green color single crystals suitable for X-ray structure determination were obtained from the filtrate after a two weeks. Yield: 74 %. Anal. Calc. for $C_{32}H_{39}N_5Ni_2O_{10}$ (771.06): C, 49.85; H, 5.10; N, 9.08 %. Found: C, 49.87; H, 5.09; N, 9.07). IR (cm^{-1}): 2967 (w), 2890 (w), 2061 (vs), 1437 (vs), 1322 (s), 1242 (s), 1208 (vs), 1055 (s), 965 (s).

*2.2.2. $[Ni_2(L^2)_2(N_3)_2(H_2O)]$ (**2**)*

This complex was synthesized following the same procedure adopted for complex **1**, using N,N-diethylethylenediammine (1 mmol, 0.118 g) instead of 2-amino-2-methyl-1-propanol. Block shaped green color single crystals suitable for X-ray diffraction were obtained after a few days. Yield: 78 %. Anal. Calc. For $C_{28}H_{44}N_{10}Ni_2O_5$ (718.15): C, 46.83; H, 6.18; N, 19.51%. Found: C, 46.79; H, 6.13; N, 19.43 (%). IR (cm^{-1}): 2973 (w), 2941 (w), 2070 (vs), 2035 (vs), 1739 (s), 1627 (s), 1441 (s), 1376 (s), 1213 (vs), 1071 (s), 956 (s), 853 (w), 743 (s).

2.3. Crystallographic data collection and refinement

Data collection for compound **1** was carried out at 173 K with Mo-Kα radiation (λ = 0.71073 Å) on a Bruker Smart ApexII CCD diffractometer, and intensities data of **2** were collected at 295 K using a Nonius Kappa CCD diffractometer with graphite monochromated Mo-Kα radiation. Structure of **1** was solved by direct methods with SHELXS-97 and refined with full-matrix least-squares SHELXL-97 [10]. For compound **2**, the data sets were integrated with the Denzo-SMN package [11] and corrected for Lorentz, polarization and absorption effects (SORTAV) [12]. The structures were solved by direct methods using SIR97 [13] system of programs and refined using full-matrix least-squares with all non-hydrogen atoms anisotropically and hydrogens included on

calculated positions, riding on their carrier atoms. All calculations were performed using SHELXL-97 [14] and PARST [15] implemented in WINGX [16] system of programs. Graphical programs used are those included in the WinGX System, [16] and Diamond [17]. Crystal data and details of refinements are given in Table 1.

2.4. Magnetic measurement

Temperature-dependent molar susceptibility measurements of polycrystalline samples were carried out at the Servei de Magnetoquímica of the CentresCientífics i Tecnològicsat the Universitat de Barcelona in a Quantum Design SQUID MPMSXL susceptometer with an applied field of 1000 and 198 G in the temperature ranges 2–300 and 2–30 K, respectively.

3. Results and discussion

3.1. Synthesis aspects

The polydentate ligands, H_2L^1 and HL^2, were prepared by a one pot synthesis employing condensation of corresponding aldehyde and ammine in methanol under reflux condition. Using these ligands, complexes **1** and **2** were synthesized at room temperature.

*3.2. Molecular structure of $[Ni_2(HL^1)_2(N_3)(C_8H_7O_3)]\cdot(H_2O)$ (**1**)*

The molecular structure of complex **1** is shown in Fig. 1 and selected bond lengths and angles are listed in Table 2. The compound crystallizes in the triclinic crystal system with P-1 space group. Complex **1** is a dinuclear nickel(II) complex with μ_2 (phenoxido) and μ_2 (azido) bridges. The dinuclear unit contains two mono deprotonated Schiff base $(H_2L^1)^-$, one 3-methoxy-2-oxo-

benzaldehyde, one azide ion with an end on ($\mu_{1,1}$) bridging mode and one water molecule as lattice solvent. Among the three phenoxide oxygens, one phenoxido oxygen, from 3-methoxy-2-oxo-benzaldehyde, O(8) acts as bridging atom between Ni(1) and Ni(2) centers and the other phenoxido oxygens (O2 and O5) from two Schiff coordinate with Ni(1) and Ni(2) atoms as terminal atom. Both the nickel(II) centers are six coordinated with distorted octahedral coordination geometries. Ni(1) centre is coordinated with bridging phenoxido oxygen (O8), bridging azido nitrogen (N1), one methoxy oxygen (O7), terminal phenoxido oxygen (O2), one imine nitrogen (N4) and one alcohol oxygen (O3). Coordination environment of Ni(2) centre contain almost identical coordinating atoms with an exception that one carbonyl oxygen atom O(9) is coordinate here instead of methoxy oxygen. The equatorial planes of Ni(1) and Ni(2) are surrounded with N(1)N(4)O(7)O(8) and N(1)N(5)O(9)O(8), respectively. Axial positions of both the nickel centers are occupied with phenoxido (O2 for Ni(1) and O5 for Ni(2)) and alcoholic oxygen (O3 for Ni(1) and O6 for Ni(2)) atoms. The nickel-oxygen bond distance ranges from 1.987(18) - 2.287(2) and 1.971(18) - 2.094(2) Å for Ni(1) and Ni(2) centers, respectively. Ni(1)-N(1) and Ni(1)-N(4) bond distances are 2.110(2) Å and 1.990(2) Å, respectively. Whereas Ni(2)-N(1) and Ni(2)-N(5) bond distances are 2.153(2) Å and 1.998(2) Å, respectively. The range of *cis* angles are 73.78(7) - 104.60(8)º and 76.64(8) – 101.78(8)º for Ni(1) and Ni(2), respectively. The *trans* angles ranges are 151.13(8) - 169.69(8)º and 164.38(8) - 175.07(8)º for Ni(1) and Ni(2) centers, respectively. The bridging Ni(1)-O(8)-Ni(2) and Ni(1)-N(1)-N(2) angles are 105.33(8)º and 96.79(8)º, respectively (Fig. 2).

*3.3. Molecular structure of [$Ni_2(L^2)_2(N_3)_2(H_2O)$](**2**)*

X-ray single crystal structure determination reveals that it consists of dinuclear nickel complex, [$Ni_2(L^2)_2(N_3)_2(H_2O)$]. The ORTEP view of the complex with atom numbering scheme is shown

in Fig.3, while the selected bond lengths and angles are given in Table 3. Complex **2** crystallizes in the orthorhombic crystal system with Pbca space group. The dinuclear unit is formed with μ_2(phenoxido) and μ_2(azido) bridges. The dinuclear unit contains two deprotonated Schiff base $(L^2)^-$, one monodentate azide, one azide with end-on ($\mu_{1,1}$) bridging mode and one coordinated water molecule. In between two $(L^2)^-$, one $(L^2)^-$ coordinate as tetra dentate ligand and coordinate with metal centers with amine nitrogen (N2), imine nitrogen (N1), phenoxido oxygen (O1) and methoxy oxygen (O2), and $(L^2)^-$ chelates two nickel centers, Ni1 with N2, N1, O1, and Ni2 with O1, O2 donor atoms. The phenoxido oxygen (O1) behaves as bridging atom between Ni1 and Ni2 centers with Ni(1)-O(1)-Ni(2) bond angle 102.51(5)°. Another $(L^2)^-$ behave as tridentate ligand and it meridionally coordinate to the Ni2 centre with its phenoxido oxygen (O3) bridge, imine nitrogen (N6) and amine nitrogen (N7) atoms. In addition to phenoxido oxygen (O1) bridge, one end on ($\mu_{1,1}$) azide also bridges two nickel centres with Ni(1)-N(8)-Ni(2) angle 98.37(7)° (Fig.4). Both the nickel centres are distorted octahedral with NiN_4O_2 and NiN_3O_3 cromophores for Ni(1) and Ni(2) centres, respectively. For Ni(1) centre the Schiff base donors N(2), N(1), O(1) and azido donor N(8) define the equatorial plane around octahedral Ni(II) ion [Ni(1)-O(1) 2.057(13), Ni(1)-N(1) 1.992(16), Ni(1)-N(2) 2.200(17), Ni(1)-N(8) 2.088(17) Å and O(1)-Ni(1)-N(2) 171.33(6)°, N(1)-Ni(1)-N(8) 164.98(7)°]. The *trans* axial positions are occupied by nitrogen (N3) from monodentate azide and water oxygen (O1W) [O(1W)-Ni(1)-N(3) 178.05(7)°]. For Ni(2) centre, the Schiff base donor O(1), O(2) from one $(L^2)^-$, N(6) from another Schiff base, and azide donor N(8) define equatorial plane [Ni(2)-O(1) 2.018(12), Ni(2)-O(2) 2.279(15), Ni(2)-N(6) 2.005(18), Ni(2)-N(8) 2.112(17) Å, O(1)-Ni(2)-N(6) 176.41(7)° and O(2)-Ni(2)-N(8) 152.86(6)°]. The *trans* axial positions are occupied by Schiff base donors O(3) and N (7) from same Schiff base and the *trans* axial angle O(3)-Ni(2)-N(7) is 167.91(6)°. The C-H…π

interactions (H(10A)···Cg(8) 2.68 Å; C(10)-H(10A)···Cg(8) 158°; C(10)···Cg(8) 3.591 Å, Table 1S) results 1D supramolecular chain like structure (Fig.1S).

3.4. Magnetic properties of complexes

Temperature-dependent magnetic susceptibility measurements of complexes **1** and **2** were carried out in the temperature range 1.9-300 K. The plots of $\chi_M T$ versus T for complexes **1** and **2** are shown in Fig.5, where χ_M is the molar magnetic susceptibility and T is the absolute temperature. The room temperature $\chi_M T$ values for both the complexes is 2.49 cm^3Kmol^{-1} which is significantly higher than the expected value for two uncoupled S = 1 spins assuming g = 2 (2.00 cm^3Kmol^{-1}). Upon cooling, $\chi_M T$ increases gradually in both cases until a maximum is reached at 30 K and 22 K for **1** and **2**, respectively. At temperatures below the maximum, $\chi_M T$ decreases abruptly from 3.21 to 1.60 cm^3Kmol^{-1} in complex **1**, and from 3.33 to 2.27 cm^3Kmol^{-1} in complex **2**, as a result of both zero-field splitting as well as possible interdimer antiferromagnetic interactions. The behaviour displayed by complexes **1** and **2**, evidence the presence of overall ferromagnetic interactions. The PHI program [18] was used to fit the experimental magnetic data. In order to avoid over parametrization during the analysis, equivalence of two Ni(II) ion is considered in the asymmetric dinuclear unit, and so one single g value for each compound was fitted. Their magnetic exchange interaction was studied with the isotropic Hamiltonian $H = -JS_1S_2$, where $S_1 = S_2 = S_{Ni}$. A zero-field splitting parameter (D) was also considered in the model in order to account for the single ion anisotropy. Additionally, an intermolecular interaction term (zJ') was also introduced in the expression. Following parameters are used to establish good agreement between the simulated curves and experimental curves: g_{Ni} = 2.13, D_{Ni} = 5.83 cm^{-1}, $J_{Ni\text{-}Ni}$ = 14.61 cm^{-1} and zJ' = -0.1 cm^{-1} for **1** and g_{Ni} = 2.15, D_{Ni} = 2.33

cm^{-1}, $J_{Ni\text{-}Ni}$ = 13.09 $cm^{-1}$and zJ' = -0.07 cm^{-1} for **2**. Temperature-independent paramagnetism (TIP) 200 × 10^{-6} cm^3mol^{-1} was considered for this system. Fig.5 shows the curves obtained from the fitting procedure are from the experimental results. The two Ni(II) ions in the complexes **1** and **2** are simultaneously bridged by a phenolate and an azide ligand, both likely mediating the magnetic exchange pathway in the molecule. It is well established in the literature that dinuclear nickel(II) compounds bridged by phenolate oxygen show antiferromagnetic behavior when the Ni-O-Ni bond angle is more than 97°, being the $J_{Ni\text{-}Ni}$ constant more negative with increasing Ni-O-Ni angle [9]. In the current compounds, this angle shows values of 105.36° and 102.51° for complexes **1** and **2**, respectively, that is significantly above the previously mentioned crossover angle. Thus, and based on the phenolate bridge only, a clear antiferromagnetic exchange should be expected in these complexes, opposite to what is experimentally observed. On the other hand, the azido bridge is coordinated to the two Ni(II) ions through the same terminal nitrogen atom, being then called end-on-azide or $\mu_{1,1}$-azido bridge. Paramagnetic metal ions bridged by $\mu_{1,1}$-N_3 show ferromagnetic exchange for a broad range of M-N-M angles [19], an increasing angle leading to a larger ferromagnetic constant [20]. The coexistence of both bridges in the same dinuclear unit represents an example of anti complementarily between ligands, in which the strong ferromagnetic exchange expected due to the azide bridge is significantly reduced through the antiferromagnetic contribution of the phenolate, as shown by our experimental results. Sasmal et al. examined possible magneto-structural correlations in heterobridged μ-phenoxo-$\mu_{1,1}$-azide dinickel(II) compounds, and among the structural factors controlling the magnitude and nature of the magnetic exchange, the authors identified the two angles previously mentioned in this paragraph and the asymmetry in bond lengths of the Ni-N-Ni bridging moiety, and some additional bond angles and lengths [5]. After extensive comparison of structural and magnetic

results, the work concluded that the global magnetic properties of this type of complexes derives from the composite effects of several structural parameters. Our results are in complete agreement with those obtained for the few similar structures reported in the literature [5, 8, 21].

4. Conclusion

We have presented here syntheses, single-crystal-structures and variable temperature magnetic behaviors of two new dinuclear μ_2-(1,1-azido) and μ_2-(1,1-phenoxido)-bridged dinuclear nickel(II) complexes **1** and **2** using Schiff bases H_2L^1 and HL^2, respectively, as chelating ligands. Variable temperature magnetic studies reveal the presence of overall ferromagnetic coupling between the nickel(II) centers in both the complexes. Magnetic properties of the complexes have been explained considering the exchange paths μ_2-(1,1-phenoxido) and μ_2-(1,1-azido). Phenoxido bridged Ni-O-Ni angles are 105.33 and 102.51°, for **1** and **2**, respectively, which favor antiferromagnetic coupling between two nickel centers. On the other hand for end-on-azido bridging the Ni-N-Ni angles are 96.79 and 98.37°, for **1** and **2**, respectively, which favor ferromagnetic coupling between two nickel centers. However ferromagnetic coupling are more dominating than antiferromagnetic coupling, which results over all ferromagnetic properties of the compounds.

Acknowledgements

The authors gratefully acknowledge the financial assistance given by the CSIR, Government of India, to Dr. Subal Chandra Manna (Project No. 01 (2743)/13/EMR-II). The authors also thank to Prof. Valerio Bertolasi (Università di Ferrara) for crystallographic contribution on complex 2. Dr. S. C. Manna thanks UGC-SAP, DST-FIST New Delhi, USIC (VU) for instrumental facilities

and Vidyasagar University for infrastructural facilities. A.F acknowledges financial support from the Spanish Ministerio de Economía y Competitividad (MINECO) through CTQ2015-68370-P, and from the regional Generalitat de Catalunya authority (2017 SGR 15). A.F is a Serra Húnter fellow.

Supplementary information

CCDC 1852544 and 1852543 contain the supplementary crystallographic data for complexes **1** and **2**. These data can be obtained free of charge via http://www.ccdc.cam.ac.uk/conts/retrieving.html, or from the Cambridge Crystallographic Data Centre, 12 Union Road, Cambridge CB2 1EZ, UK; fax: (+44) 1223-336-033; or e-mail: deposit@ccdc.cam.ac.uk. IR and electronic spectral results have also been deposited.

References

[1] (a) P. Mukherjee, M. G. B. Drew, C. J. Gomez-García, A. Ghosh, Inorg. Chem. 48 (2009) 4817 - 4827; (b) P. Mukherjee, M. G. B. Drew, C. J. Gomez-Garcıía, A. Ghosh, Inorg. Chem. 48 (2009) 5848 - 5860; (c) J. Esteban, M. Font-Bardia, J. S. Costa, S. J. Teat, A. Escuer, Inorg. Chem. 53 (2014) 3194 - 3203; (d) S. Khanra, T. Weyhermu1ller, E. Rentschler, P. Chaudhuri, Inorg. Chem. 44 (2005) 8176-8178.

[2] (a) S. Petit, P. Neugebauer, G. Pilet, G. Chastanet, A.-L. Barra, A. B. Antunes, W. Wernsdorfer, D. Luneau, Inorg. Chem. 51 (2012), 6645 - 6654; (b) A. Ferguson, J. Lawrence, A. Parkin, J. Sanchez-Benitez, K. V. Kamenev, E. K. Brechin, W. Wernsdorfer, S. Hill, M. Murrie,

Dalton Trans. (2008) 6409 - 6414; (c) G. Rajaraman, K. E. Christensen, F. K. Larsen, G. A. Timco, R. E. P. Winpenny, Chem. Commun. (2005) 3053 - 3055.

[3] F. Meyer, E. Kaifer, P. Kircher, K. Heinze, H. Pritzlow, Chem. Eur. J. 5 (1999) 1617 -1630.

[4] (a) D. Volkmer, B. Hommerich, K. Griesar, W. Haase, B. Krebs, Inorg. Chem. 35 (1996) 3792 -3803; (b) A. M. Barrios, S. J. Lippard, Inorg. Chem. 40 (2001) 1250 -1255; (b) R. Biswas, S. Mukherjee, P. Kar, A. Ghosh, Inorg. Chem. 51 (2012) 8150 - 8160.

[5] S. Sasmal, S. Hazra, P. Kundu, S. Dutta, G. Rajaraman, E. C. Sanudo, S. Mohanta, Inorg. Chem. 50 (2011) 7257 -7267.

[6] (a) S. C. Manna, S. Konar, E. Zangrando, M. G. B. Drew, J. Ribas, N. Ray Chaudhuri, Eur. J. Inorg. Chem. (2005) 1751 -1758; (b) Molecular-Based Magnetic Materials: Theory, Technique and Applications (Eds.: M. M. Turnbull, T. Sugimoto, L. K. Thomson), ACS Symposium Series 644, American Chemical Society: Washington DC, (1996); (c) D. Gatteschi, O. Kahn, J. S. Miller, F. Palacio, Magnetic Molecular Materials; NATO ASI, Kluwer: Dordrecht (1991); (e) M. A. Halcrow, J. C. Huffman, G. Christou, Angew. Chem. Int. Ed. Engl. 34 (1995) 889 - 891; (f) M. Monfort, I. Resino, J. Ribas, H. Stoeckli-Evans, Angew. Chem. Int. Ed. 39 (2000) 191 - 193.

[7] (a) M. I. Arriortua, A. R. Cortes, L. Lezama, T. Rojo, X. Solans, Inorg. Chim. Acta 174 (1990) 263; (b) A. Escuer, R. Vicente, J. Ribas. J. Magn. Mater. 110 (1992) 181-184; (c) A. Escuer, R. Vicente, J. Ribas, X. Solans. Inorg. Chem. 34 (1995) 1793 - 1798.

[8] R. Koner, S. Hazra, M. Fleck, A. Jana, C. R. Lucas, S. Mohanta, Eur. J. Inorg. Chem. (2009) 4982-4988.

[9] (a) X.-H. Bu, M. Du, L. Zhang, D.-Z. Liao, J.-K. Tang, R.-H. Zhang, M. Shionoya, J. Chem. Soc., Dalton Trans. (2001), 593-598; (b) A. Burkhardt, E. T. Spielberg, S. Simon, H. Gçrls, A.

Buchholz, W. Plass, Chem. Eur. J. 15 (2009) 1261-1271; (c) R. Biswas, S. Giri, S. K. Saha, A. Ghosh, Eur. J. Inorg. Chem. (2012) 2916-2927.

[10] A short history of SHELX. Sheldrick, G. M. Acta Cryst. A64 (2008) 112 - 122.

[11] Z. Otwinowski, W. Minor, Methods in Enzymology, Part A, ed. C. W. Carter and R. M. Sweet, Academic Press, London, vol. 276 (1997) p. 307.

[12] R. H. Blessing, Acta Crystallogr., Sect. A: Found. Crystallogr. 51 (1995) 33-33.

[13] A. Altomare, M. C. Burla, M. Camalli, G. L. Cascarano, C. Giacovazzo, A. Guagliardi, A. G. Moliterni, G. Polidori and R. Spagna, J. Appl. Crystallogr. 32 (1999) 115-119.

[14] G. M. Sheldrick, SHELX-97, Program for Crystal Structure Refinement, University of Gottingen, Germany (1997).

[15] M. Nardelli, J. Appl. Crystallogr. 28 (1995) 659.

[16] L. J. Farrugia, J. Appl. Crystallogr. 32 (1999) 837-837.

[17] K. Brandenburg, DIAMOND (version 3.2i), Crystal Impact GbR, Bonn, Germany (1999).

[18] N. F. Chilton, R. P. Anderson, L. D. Turner, A. Soncini and K. S. Murray, J. Comput. Chem. 34 (2013) 1164 - 1175.

[19] E. Ruiz, J. Cano, S. Alvarez, P. Alemany, J. Am. Chem. Soc. 120 (1998) 11122 -11129.

[20] (a) P. Chaudhuri, R. Wagner, S. Khanra, T. Weyhermuller, Dalton Trans. (2006) 4962 - 4968; (b) G. Manca, J. Cano, E. Ruiz, Inorg. Chem. 48 (2009) 3139–3144.

[21] (a) S. K. Dey, N. Mondal, M. S. El Fallah, R. Vicente, A. Escuer, X. Solans, M. Font-Bardía, T. Matsushita, V. Gramlich, S. Mitra, Inorg. Chem. 43 (2004) 2427-2434; (b) A. Banerjee, R. Singh, D. Chopra, E. Colacio, K. K. Rajak, Dalton Trans. (2008) 6539 -6545; (c) P. P. Chakrabarty, S. Giri, D. Schollmeyer, H. Sakiyama, M. Mikuriya, A. Sarkar, S. Saha,

Polyhedron 89 (2015) 49–54; (d) P. Ghorai, A. Chakraborty, A. Panja, T. K. Mondala, A. Saha, RSC Adv. 6 (2016) 36020 - 36030.

Table 1 Crystal data and structure refinement for complexes **1** and **2**.

Complex	**1**	**2**
Empirical formula	$C_{32}H_{39}N_5Ni_2O_{10}$	$C_{28}H_{44}N_{10}Ni_2O_5$
Formula mass, g mol^{-1}	771.06	718.15
Crystal system	Triclinic	Orthorhombic
Space group	P-1	Pbca
a, Å	10.0846(6)	12.4197(1)
b, Å	12.5179(7)	21.4737(4)
c, Å	14.1176(8)	24.4569(5)
α, deg	74.3873(7)	90
β, deg	83.9553(7)	90
γ, deg	83.1921(7)	90
Z	2	8
V, Å^3	1699.29(17)	6522.58(19)
$D_{(calcd)}$, g cm^{-3}	1.507	1.463
μ(Mo-Ka), mm^{-1}	1.172	1.208
F(000)	804	3024
Theta range, deg	2.4, 28.0	2.5, 28.0
No.of collected data	9843	38122
No. of unique data	7455	7820
R_{int}	0.015	0.044
h,k,lmax	12, 16, 18	16, 28, 32
Observed reflections [$I > 2\sigma(I)$]	5990	6129
Goodness of fit (F^2)	1.04	1.02
*R*1, *wR*2 (all data) [a]	0.0402, 0.1021	0.0349, 0.0895
Residuals, e Å^{-3}	-0.39, 0.80	-0.36, 0.31

[a] $R1(Fo) = \Sigma \| \|Fo\| - \|Fc\| \| / \Sigma |Fo|$, $wR2(Fo^2) = [\Sigma w (Fo^2 - Fc^2)^2 / \Sigma w (Fo^2)^2]^{½}$

Table 2 Experimental coordination bond lengths (Å) and angles (°) for complex **1**.

Bond lengths			
Ni(1)-O(2)	1.9875(18)	Ni(2)-O(5)	1.9714(18)
Ni(1)-O(3)	2.097(2)	Ni(2)-O(6)	2.094(2)
Ni(1)-O(7)	2.287(2)	Ni(2)-O(8)	2.0034(19)
Ni(1)-O(8)	2.0052(18)	Ni(2)-O(9)	2.088(2)
Ni(1)-N(1)	2.110(2)	Ni(2)-N(1)	2.153(2)
Ni(1)-N(4)	1.990(2)	Ni(2)-N(5)	1.998(2)
Bond angles			
O(2)-Ni(1)-O(3)	169.69(8)	O(5)-Ni(2)-O(6)	172.94(8)
O(2)-Ni(1)-O(7)	84.14(7)	O(5)-Ni(2)-O(8)	92.41(8)
O(2)-Ni(1)-O(8)	99.81(7)	O(5)-Ni(2)-O(9)	92.84(8)
O(2)-Ni(1)-N(1)	97.24(8)	O(5)-Ni(2)-N(1)	91.08(8)
O(2)-Ni(1)-N(4)	92.49(8)	O(5)-Ni(2)-N(5)	92.29(8)
O(3)-Ni(1)-O(7)	90.29(8)	O(6)-Ni(2)-O(8)	94.38(8)
O(3)-Ni(1)-O(8)	86.89(8)	O(6)-Ni(2)-O(9)	85.45(8)
O(3)-Ni(1)-N(1)	91.83(8)	O(6)-Ni(2)-N(1)	92.39(8)
O(3)-Ni(1)-N(4)	80.44(8)	O(6)-Ni(2)-N(5)	80.98(8)
O(7)-Ni(1)-O(8)	73.78(7)	O(8)-Ni(2)-O(9)	88.09(8)
O(7)-Ni(1)-N(1)	151.13(8)	O(8)-Ni(2)-N(1)	76.64(8)
O(7)-Ni(1)-N(4)	104.15(8)	O(8)-Ni(2)-N(5)	175.07(8)
O(8)-Ni(1)-N(1)	77.60(8)	O(9)-Ni(2)-N(1)	164.38(8)
O(8)-Ni(1)-N(4)	167.17(8)	O(9)-Ni(2)-N(5)	93.17(8)
N(1)-Ni(1)-N(4)	104.60(8)	N(1)-Ni(2)-N(5)	101.78(8)
Ni(1)-O(8)-Ni(2)	105.33(8)		
Ni(1)-N(1)-Ni(2)	96.79(8)		

Table 3 Experimental coordination bond lengths (Å) and angles (°) for complex **2**.

Bond lengths			
Ni(1)-O(1)	2.0576(13)	Ni(2)-O(1)	2.0186(12)
Ni(1)-O(1W)	2.1830(17)	Ni(2)-O(2)	2.2793(15)
Ni(1)-N(1)	1.9925(16)	Ni(2)-O(3)	2.0278(15)
Ni(1)-N(2)	2.2000(17)	Ni(2)-N(6)	2.0055(18)
Ni(1)-N(3)	2.0761(17)	Ni(2)-N(7)	2.1722(17)
Ni(1)-N(8)	2.0888(17)	Ni(2)-N(8)	2.1120(17)
Bond angles			
O(1)-Ni(1) –O(1W)	86.40(6)	O(1)-Ni(2)-O(2)	74.12(5)
O(1)-Ni(1)-N(1)	88.65(6)	O(1)-Ni(2)-O(3)	88.32(5)
O(1)-Ni(1)-N(2)	171.33(6)	O(1)-Ni(2)-N(6)	176.41(7)
O(1)-Ni(1)-N(3)	92.97(6)	O(1)-Ni(2)-N(7)	101.74(6)
O(1)-Ni(1)-N(8)	78.65(6)	O(1)-Ni(2)-N(8)	78.98(6)
O(1W)-Ni(1)-N(1)	85.89(6)	O(2)-Ni(2)-O(3)	82.31(6)
O(1W)-Ni(1)-N(2)	87.45(6)	O(2)-Ni(2)-N(6)	105.49(7)
O(1W)-Ni(1)-N(3)	178.05(7)	O(2)-Ni(2)-N(7)	93.90(6)
O(1W)-Ni(1)-N(8)	85.35(6)	O(2)-Ni(2)-N(8)	152.86(6)
N(1)-Ni(1)-N(2)	84.81(7)	O(3)-Ni(2)-N(6)	88.10(7)
N(1)-Ni(1)-N(3)	92.25(7)	O(3)-Ni(2)-N(7)	167.91(6)
N(1)-Ni(1)-N(8)	164.98(7)	O(3)-Ni(2)-N(8)	93.54(6)
N(2)-Ni(1)-N(3)	92.97(6)	N(6)-Ni(2)-N(7)	81.84(7)
N(2)-Ni(1)-N(8)	106.94(6)	N(6)-Ni(2)-N(8)	101.14(7)
N(3)-Ni(1)-N(8)	96.34(7)	N(7)-Ni(2)-N(8)	94.95(7)
Ni(1)-O(1)-Ni(2)	102.51(5)		
Ni(1)-N(8)-Ni(2)	98.37(7)		

Caption of the Figures

Fig.1. ORTEP drawing (ellipsoid probability 30%) of complex **1** with atom labels.

Fig. 2. Molecular structure of complex **1** showing bridging angles (hydrogen atoms are excluded for clarity).

Fig. 3. ORTEP drawing (ellipsoid probability 30%) of complex **2** with atom labels.

Fig. 4. Molecular structure of complex **2** showing bridging angles (hydrogen atoms are excluded for clarity).

Fig.5. Thermal dependence of the $\chi_M T$ for complexes **1** and **2**. The straight lines represent the fits of the experimental data considering a Ni(II) homodinuclear magnetic model and using the parameters mentioned in the text.

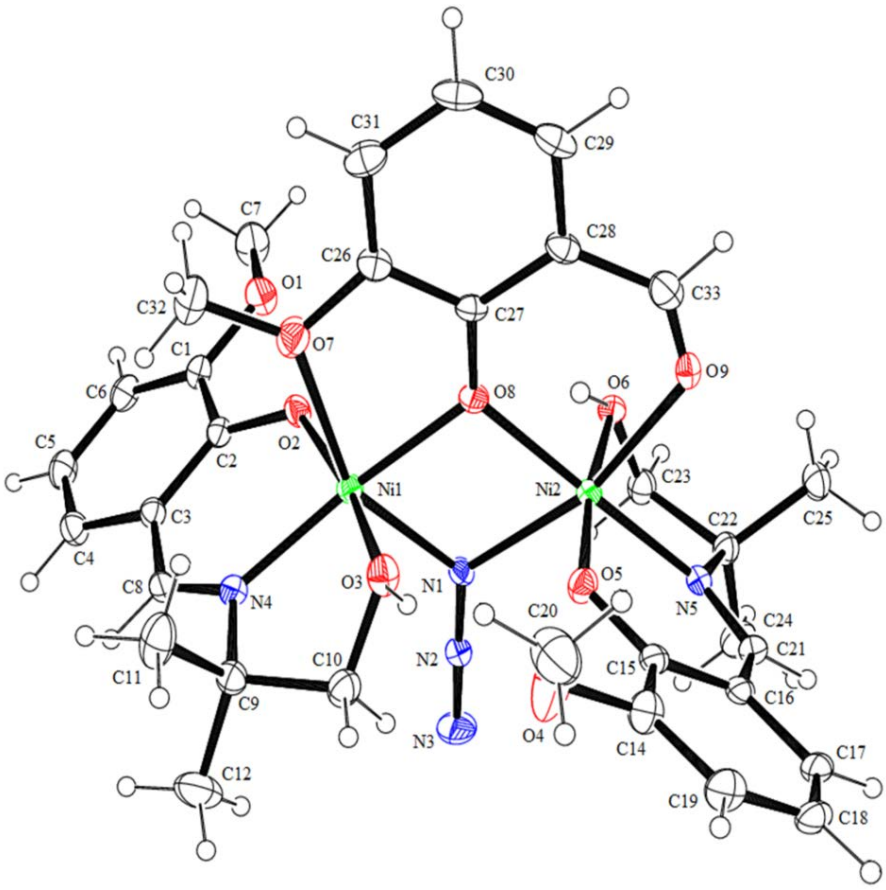
C30
C31
C29
C7
C28
C26
O1
C33
C32
C27
O7
C1
O9
C6
O8
O6
O2
C5
C2
Ni1
Ni2
C23
C3
C22
C25
C4
C8
O3
N1
O5
N4
N5
C20
C24
C21
C11
C10
N2
C15
C16
C9
O4
N3
C14
C17
C12
C19
C18

Fig.1

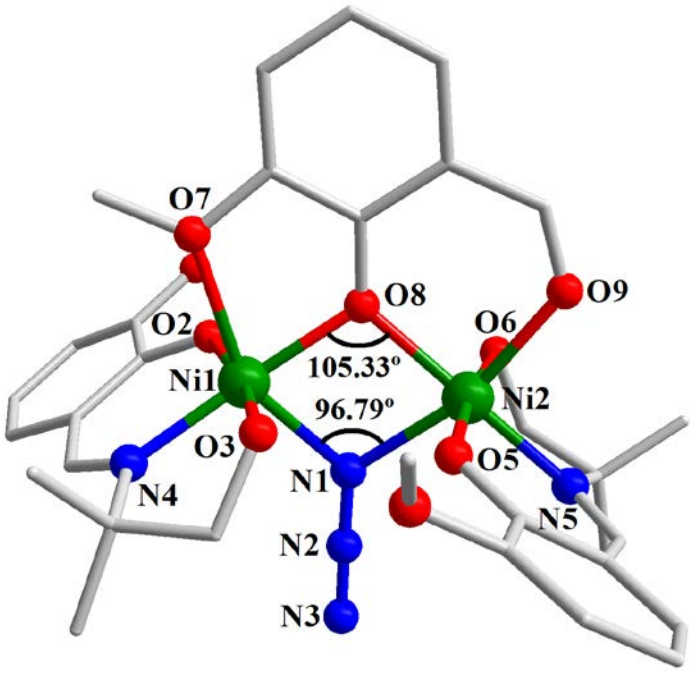
O7
O8
O9
O2
O6
105.33°
Ni1
96.79°
Ni2
O3
O5
N1
N4
N5
N2
N3

Fig. 2

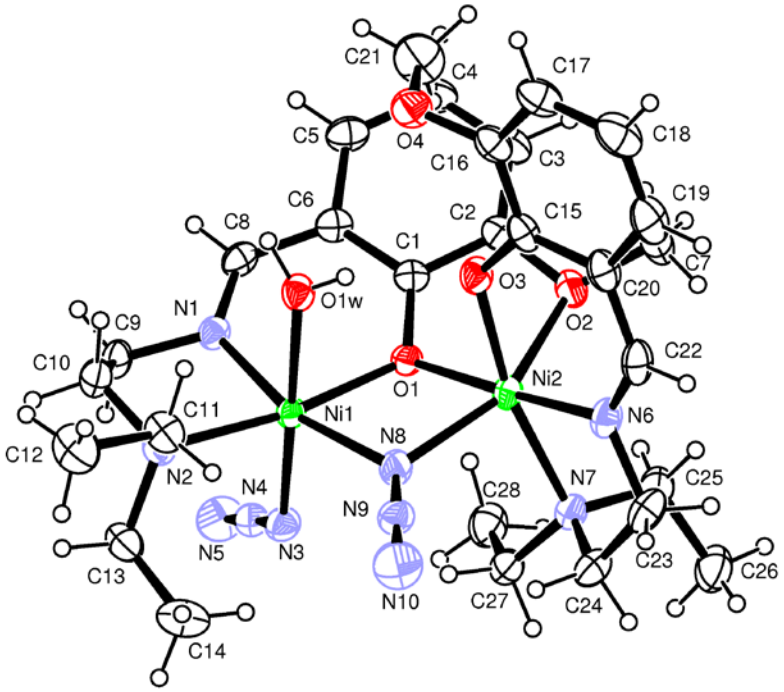
C21
C4
C17
C5
O4
C16
C3
C18
C6
C2
C15
C19
C8
C1
C7
O1w
O3
O2
C20
N1
C9
C10
O1
Ni2
C22
C11
Ni1
N8
N6
C12
N2
N4
N7
C25
C28
N9
N5
N3
C23
C26
C13
N10
C27
C24
C14

Fig. 3

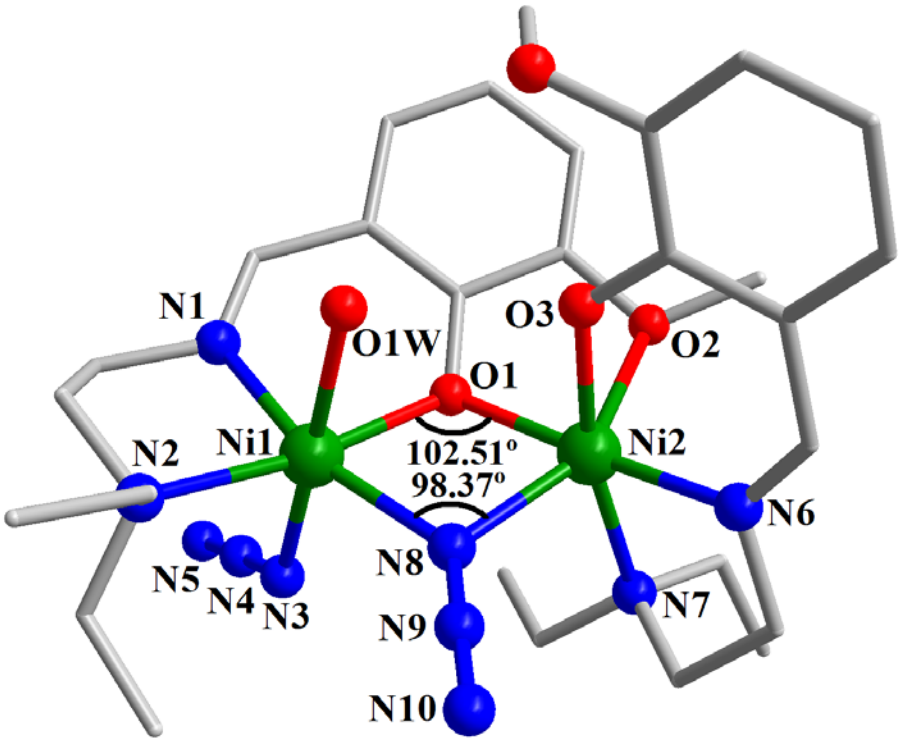

Fig. 4

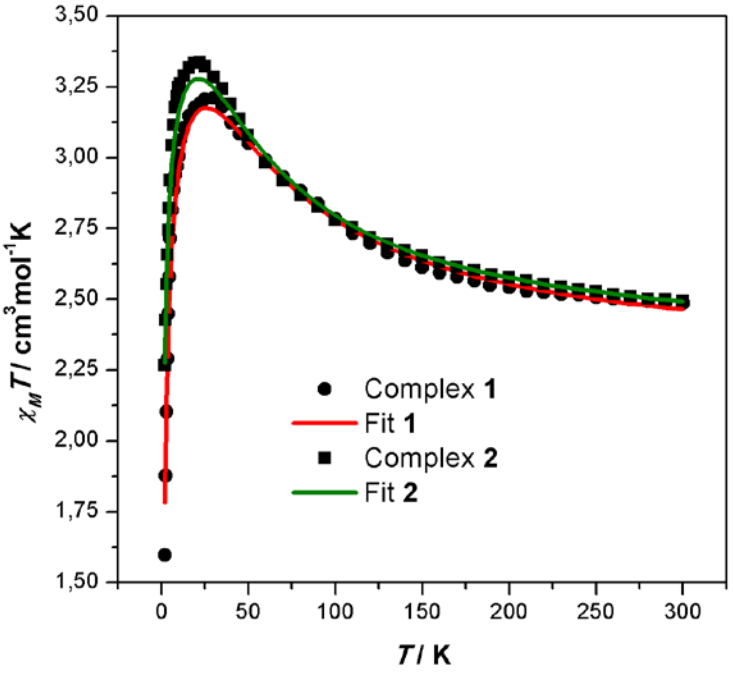
3,50
3,25
3,00
2,75
2,50
2,25
2,00
1,75
1,50
0
50
100
150
200
250
300
$\chi_M T$ / cm^{3}mol^{-1}K
T / K
Complex 1
Fit 1
Complex 2
Fit 2

Fig.5